The Sensitivity of the Mid-21st Century Cold Season Hydroclimate in California to Global Warming: An RCM Projection Based on NCAR CCSM3 Projection with the SRES-A1B Emission Scenarios

Kim, J.[1], D. Waliser[2], R. Fovell[1], A. Hall[1], K. Liou[1], J. McWilliams[1], Y. Xue[1], Sarah Kapnick[1], A. Eldering[2], Y. Chao[2], and Q. Li[1]

[1] University of California, Los Angeles [2] Jet Propulsion Laboratory/Caltech/NASA

http://www.jifresse.ucla.edu

1. Introduction

Observational and modeling studies strongly suggests that significant global climate change induced by the increase in greenhouse gases (GHGs) will occur in this century. Future changes in the regional hydroclimate in response to the global change is an important concern in California that is characterized by extreme contrasts in precipitation with wet cold seasons and dry warm seasons. California relies heavily on cold season precipitation and snow accumulation for the water supply in the dry warm seasons. Observational studies (e.g., Dettinger and Cayan 1995; Stewart et al. 2005) revealed that global climate change appears to be affecting the snowpack and snowmelt-driven runoff in California's mountainous region. The water supply in California has been marginal for supporting its large population and industries, especially agriculture. Thus, reliable assessments of the impact of the climate change on the future water resources in the region has been an important concern to the water managers in California (Anderson et al. 2008) . This being said, the amplitude and consequences of the changes to the global climate are still far from certain, particularly on regional and local scales. To illustrate, **Figure 1.1a** shows projections of the annual mean surface air temperature (SAT) change for southern/central California from 18 different global climate models (GCMs) that have contributed to the 4th Assessment Report of the Intergovernmental Panel on Climate Change (IPCC). Noteworthy is the fact that every model predicts increases in SAT for this region, albeit with an uncertainty factor of 3 at the end of the 21st century. More problematic for determining the consequences to society, agriculture, ecosystem viability, etc. are the associated projections for precipitation change that are shown in **Figure 1.1b**. In this case, the models are not even in agreement whether California will become wetter or drier with the uncertainty ranging up to +/- 20% of the annual mean rainfall.

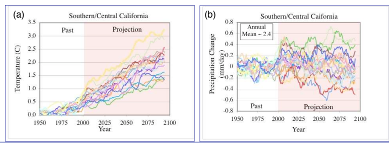

Figure 1.1 Model simulations of the changes in annual mean surface air temperature (left) and precipitation (right) for Southern/Central California relative to a climatology calculated for the period 1900-1999. Each line represents a different GCM contribution (N=17) for the IPCC's 4th Assessment Report (2007). The period up to 2000 is based on simulations using "known" 20th century GHG forcing conditions, while the period after is based on "projected" (i.e. SRESA1B scenario) GHG forcing conditions.

A considerable part of the uncertainty and disagreement in **Figure 1.1, especially precipitation,** lies in the fact that the global models poorly, or do not, resolve important physical processes and terrain variations that are fundamental for a realistic simulation for regional scales. To illustrate, **Figure 1.2** compares a global SAT map for Jan 1999 from one of the GCMs in **Figure 1.1** and the MODIS-derived SAT. Also shown in the figure is false-color images for an embedded sub-domain in the region. Evident is the extremely rich environmental structure that includes variability in atmospheric (e.g. clouds), oceanic (e.g., temperature and Chl), and land surface (e.g., topography, vegetation types, snow cover) processes at very fine spatial scales (Dx ~ 1km). This structure is simply not represented by the GCMs. This is a crucial problem in California in which spatial distribution of precipitation is strongly correlated with the complex terrain in the region.

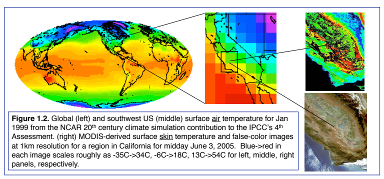

Figure 1.2. Global (left) and southwest US (middle) surface air temperature for Jan 1999 from the NCAR 20th century climate simulation contribution to the IPCC's 4th Assessment. (right) MODIS-derived surface skin temperature and false-color images at 1km resolution for a region in California for midday June 3, 2005. Blue->red in each image scales roughly as -35C->34C, -6C->18C, 13C->54C for left, middle, right panels, respectively.

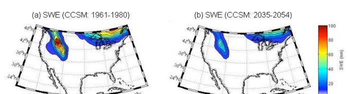

Figure 1.3. The snow-water equivalence (SWE) in the present-day and mid-20th century periods in the CCSM simulation.

The lack of spatial resolution and the associated inadequate representation of orography in global models tend to result in substantial errors in surface hydrologic fields. An example is shown in Figure 1.3; The NCAR-CCSM3 could not resolve the Sierra Nevada and the snow pack in the region.

To address the above needs, the UCLA Joint Institute for Regional Earth System Science and Engineering (JIFRESSE), a collaboration between UCLA and the Jet Propulsion Laboratory (JPL) to improve understanding and to develop projections of the impact of global climate change on regional climates and environments, has developed a comprehensive Regional Earth System Model (RESM) that contains advanced treatments of the physical and dynamical processes in the atmosphere, coastal ocean, and land-surface (**Figure 1.4**). The RESM is based on one-way and/or interactive nesting of the models for limited-area atmosphere (WRF), ocean (ROMS) and air quality (CMAQ).

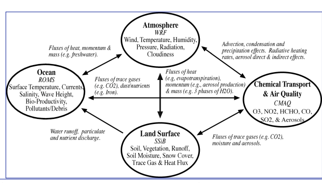

Figure 1.4 Schematic representation of the coupled regional Earth System model configuration, including advanced modeling components for the Atmosphere (WRF), Land Surface (SSiB), Chemical Transport and Air Quality (CMAQ) and the Ocean (ROMS).

This study investigates the impact of the climate change induced by increased GHGs on the surface hydroclimate in California by dynamically downscaling a global climate scenario generated by the NCAR CCSM3 on the basis the IPCC SRES-A1B emission profile. Details on the experiment are presented in Section 2. Section 3 present the climate change signals in the key surface hydroclimate during the cold season.

2. Experimental Design

The dynamical downscaling is performed using the Weather Research and Forecast (WRF) model, version 2.2.1 (Skamarock et al. 2005). The model solves a non-hydrostatic momentum equation in conjunction with thermodynamic energy equation. Numerically, the model features multiple options for the advection scheme and the parameterized atmospheric physical processes. In conjunction with one-way and/or interactive self nesting capability, this allows us to apply the model to simulate atmospheric circulation of a wide range of spatial scales. More details of the WRF model can be found in the web site http://wrf-model.org. The physics options selected in this experiment includes the NOAH land-surface scheme (Chang et al. 1999), the simplified Arakawa Schubert (SAS) convection scheme (Hong and Pan 1998), the RRTM longwave radiation scheme Mlawer et al. 1997), Dudhia (1989) shortwave radiation, and the WSM 3-class with simple ice cloud microphysics scheme. For more details on the physics options, readers are referred to the web site http://wrf-model.org.

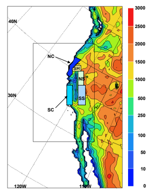

Figure 2.1 The model domain and the terrain (m) represented at the 36km resolution.

The domain covers the western United States (WUS) region at a 36km resolution and 27 sigma layers. The inner box shows the California region for which the results are presented. At this horizontal resolution, the model terrain captures major orographic variations in the WUS region; however, the high elevation regions in the Sierra Nevada and the narrow but steep coastal terrain is somewhat under-represented.

Also shown in Figure 2.1 are the 5 sub-regions, Northern Coastal Range (NC), Southern Coastal Range (SC), Mt Shasta (SH), Northern Sierra Nevada (NS0, and Southern Sierra Nevada (SS), selected for more detailed spatial variations in the projected climate change signals within California. Among these sub-regions, the three regions, SH, NS, and SS feeds most of the major reservoirs that supplies water in California. The wettest region in California (the Smith River basin) is located in the northern end of NC.

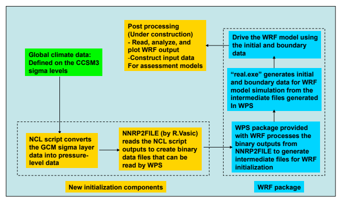

Figure 2.2 The data flow in the regional climate change projection

The regional climate simulations are driven by the global climate data by the NCAR CCSM3 that is generated according to the SRES-A1B emission profile (Nakicenovic et al. 2000). The emission scenario assumes balanced energy generation between fossil and non-fossil fuel; the resulting CO_2 emissions is located near the averages of all SRES emission scenarios. The climatology for the late 20th century and mid-21st century periods is calculated from the 20 cold season regional simulations for 1961-1980 and 2035-2054, respectively. The cold season covers the 6-mo period Oct-Mar and includes two seasons; fall (OND) and Winter (JFM). The CO_2 concentrations in the WRF simulations have been fixed at 330ppmv and 430ppmv during the present-day and mid-21st century periods, respectively.

3. Results

Figure 3.1 Low-level air temperature

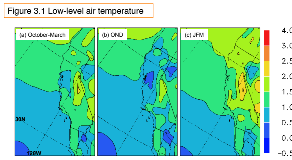

Figure 3.1 The projected climate change signal shows that the low-level air temperature will increase in California by 1-2.5K with noticeable variations according to geography and season. Seasonally, the temperature signals are larger in winter (Fig. 3.2c) than in fall (Fig. 3.2b). Geographically, the projected warming signals vary according to latitudes, the distance from the coastline, and terrain elevation. The warming signals increase towards the north and away from the ocean. The warming signals also vary according to terrain elevation with the largest warming signals occurring in the high elevation Sierra Nevada region.

Figure 3.2 Surface albedo

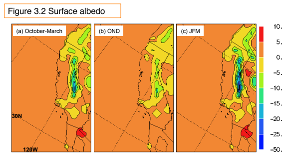

Figure 3.2 The projected changes in surface albedo decreases significantly in the high elevation regions in northern California and the Sierra Nevada. The changes in albedo are negligible in low elevation regions. The decrease in surface albedo is more pronounced in winter than in fall as well. In conjunction with the changes in snowfall and snowpack shown in Figure 3.6, the results show that the projected temperature change in the high elevation regions are partially augmented by local snow-albedo feedback.

Figure 3.3 Precipitation: % changes

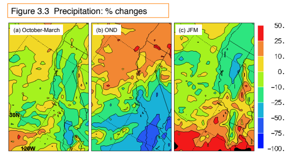

Figure 3.3 The precipitation change signals also vary according to geography and season. In the early part of the cold season (i.e., fall), positive precipitation changes in northern California are contrasted by negative precipitation in southern California. This north-south pattern is reversed in winter. For the entire cold season, precipitation decreases in the entire California region.

Figure 3.4 Rainfall: % changes

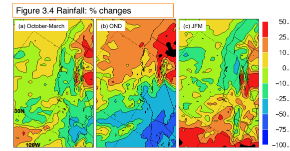

Figure 3.4 The spatial variations in the seasonal precipitation changes are associated chiefly with the rainfall changes. One exception is in the northern Sierra Nevada region where rainfall increases in both seasons. The increase in rainfall in the region is one of the most important consequences of the low level warming; converting snowfall in colder climate into rainfall in warmer climate.

Figure 3.5 Snowfall: % changes

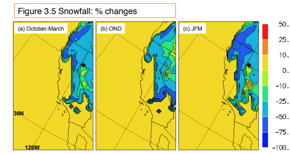

Figure 3.5 Snowfall decreases everywhere in California except in a small region in the Sierra Nevada where the model terrain exceeds 2500m during winter. In this very high elevation region, the winter snowfall change signals ranges between 10 and 25% of the control climate. This result is consistent with the previous study by Kim (2001) whose study also projects the increase in snowfall in parts of the Sierra Nevada region where the model terrain exceeds 2500m. This area of high elevation region is very small and the projected snowfall decreases substantially in most high elevation regions where the snowmelt driven warm season runoff originates.

Figure 3.6 SWE: % changes

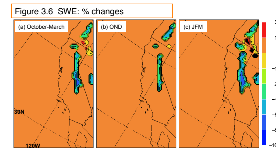

Figure 3.7 Runoff: % changes

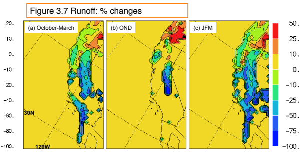

Figures 3.6 and 3.7 shows that in response to the changes in precipitation characteristics (Figure 3.4 and 3.5), the seasonal mean SWE and runoff in high elevation regions decrease substantially in the warmer climate. The decreases are more notable in winter. The decrease in winter SWE will exert an adverse impact on the warm season water supply in the region

Table 1. The climate change signals defined as the differences in the model climatology between the mid-21st century (2035-2054) and the late 20th century (1961-1980) in key surface hydrologic variables. The numbers in the parenthesis indicate the climate change signals in terms of the percent of the late 20th century RCM climatology. The percent change in snowfall and snowmelt over the SC region is not defined due to very small local snowfall in both the control and mid-century periods.

	Season	NC	SC	SH	NS	SS
Precipitation (mm/mo)	Fall (OND)	22.5 (11.5)	-6.6 (-11.7)	23.5 (15.2)	16.1 (9.85)	-16.0 (-15.4)
	Winter (JFM)	-64.4 (-21.5)	-15.1 (-14.6)	-44.8 (-17.2)	-82.6 (-26.6)	-39.8 (-20.9)
	Oct-Mar	-21.0 (-8.46)	-10.9 (-13.6)	-10.7 (-5.2)	-33.2 (-14.0)	-27.9 (-19.0)
Rainfall (mm/mo)	Fall (OND)	25.4 (13.5)	-6.7 (-12.2)	34.8 (28.0)	29.6 (22.7)	-3.6 (-5.1)
	Winter (JFM)	-54.7 (-19.4)	-15.5 (-15.0)	-14.0 (-6.93)	-45.8 (-19.1)	-12.2 (-10.7)
	Oct-Mar	-14.6 (-6.23)	-11.2 (-14.0)	-10.4 (6.4)	-8.1 (-4.4)	-7.9 (-8.6)
Snowfall (mm/mo)	Fall (OND)	-2.9 (-41.7)	0.2 (n/a)	-11.3 (-40.5)	-13.5 (-40.5)	-12.5 (-36.5)
	Winter (JFM)	-9.7 (-53.1)	0.4 (n/a)	-30.8 (-51.3)	-36.8 (-52.6)	-27.6 (-36.5)
	Oct-Mar	-6.3 (-50.0)	0.3 (n/a)	-21.1 (-46.9)	-25.1 (-48.7)	-20.0 (36.5)
Runoff (mm/mo)	Fall (OND)	-0.1 (-0.4)	-0.2 (-11.2)	-0.7 (5.6)	-1.9 (-10.7)	-6.5 (-63.1)
	Winter (JFM)	-12.9 (-10.4)	-3.4 (-28.2)	-3.6 (-3.8)	-24.9 (-22.6)	-16.5 (-29.4)
	Oct-Mar	-6.5 (-50.0)	-1.78 (-26.7)	-1.4 (-2.7)	-13.4 (-21.0)	-11.5 (-34.6)
Snowmelt (mm/mo)	Fall (OND)	-2.89 (-42.0)	0.2 (n/a)	-10.1 (-36.4)	-11.3 (-37.7)	-8.5 (-29.9)
	Winter (JFM)	-9.75 (-52.8)	0.4 (n/a)	-32.3 (-51.9)	-39.4 (-54.0)	-30.7 (-38.6)
	Oct-Mar	-6.32 (-50.0)	0.3 (n/a)	-21.2 (-47.2)	-25.4 (-49.2)	-19.6 (-36.3)
SWE (mm)	Fall (OND)	0.1 (42.3)	0.0 (0.0)	-1.1 (-32.9)	-1.4 (29.9)	-3.1 (-42.7)
	Winter (JFM)	-1.3 (-78.5)	0.0(0.0)	-2.9 (-58.1)	-5.0 (-65.5)	-13.2 (-67.9)
	Oct-Mar	-0.6 (-60.8)	0.0 (0.0)	-3.2 (-52.0)	-3.21 (-52.0)	-8.2 (-61.1)
T2 (C)	Fall (OND)	0.87	0.59	0.95	0.98	1.38
	Winter (JFM)	1.73	1.42	1.77	1.94	2.09
	Oct-Mar	1.30	1.36	1.36	1.46	1.74

Conclusions

(1) The low-level air temperature will increase by 1-2.5K, with larger increases in high elevation regions during the late half of the cold season (winter). The geographical variations in the projected warming signals are associated with the significant depletion of snowpack in the warmer climate and the prevailing westerlies.
(2) Surface albedo decreases notably in high elevation regions in northern California and the Sierra Nevada. The decrease in the surface albedo is more pronounced in winter than in fall because the depletion of snowpack is larger in winter than in fall.
(3) The cold season precipitation decreases in the entire region of California. The precipitation changes show strong interseasonal variations: Fall precipitation increases in the northern California and decreases in the southern California region. The winter precipitation changes show opposite features with increases (decreases) in the southern (northern) California region.
(4) Rainfall increases notably in the high elevation regions in the northern Sierra Nevada where a significant portion of snowfall in the present-day climate falls as rain in the warmer climate due to higher freezing level altitudes.
(5) Snowfall decreases throughout the cold season by 25-50% of the amount in the present-day climate. The largest percent-decrease in snowfall occurs in the Mt. Shasta and the northern Sierra Nevada regions during the late part of the cold season (winter).
(6) The snowpack in the high elevation Mt. Shasta and the Sierra Nevada regions decrease by over 40% in fall and nearly 70% in winter due to reduced snowfall. The reduced snowfall in the warmer climate also results in the reduction in snowmelt by 38% and 54% of the late 20th century values during fall and winter, respectively.
(7) The cold season runoff decreases in California due to reduced precipitation.

The climate change signals obtained in this study, especially the reduction in high elevation snowpack, suggests that the climate change will adversely affect the water resources in California.

It must be noted that the results in this study represent only one of many global climate change scenarios that are equally plausible. The changes in the key surface hydroclimate fields projected in this study compares qualitatively with the results in previous studies (Leung and Ghan 1999; Kim et al. 2002); however, details in the projected climate change signals vary among these studies primarily due to the differences in the GCM climate projections used to drive an RCM.

Acknowledgement

The research described in this paper was performed as an activity of the Joint Institute for Regional Earth System Science and Engineering, through an agreement between the University of California, Los Angeles, and the Jet Propulsion Laboratory, California Institute of Technology, and was sponsored by the National Aeronautics and Space Administration. Preprocessing of the CCSM data was also partially funded by National Institute of Environmental Research, Korea.